Dalton Transactions

Cite this: *Dalton Trans.*, 2011, **40**, 8664

www.rsc.org/dalton

PAPER

Metal-promoted synthesis of amidines containing the model nucleobases 1-methylcytosine and 9-methyladenine†

Diego Montagner,*[a] Ennio Zangrando,[b] Giuseppe Borsato,[c] Vittorio Lucchini[c] and Bruno Longato[a]

Received 12th April 2011, Accepted 8th June 2011
DOI: 10.1039/c1dt10638d

The amidine complexes *cis*-[L_2PtNH=C(R){1-MeCy(-2H)}]NO_3 (R = Me, **1a**; Ph, **1b**, Me_3C, **1c**; Ph_2(H)C, **1d**) and *cis*-[L_2PtNH=C(R){9-MeAd(-2H)}]NO_3 (R = Me, **2a**; Ph, **2b**; Me_3C, **2c**; Ph_2(H)C, **2d**), are formed when *cis*-[L_2Pt(μ-OH)]$_2$(NO_3)$_2$ (L = PPh_3) reacts with 1-methylcytosine (1-MeCy) and 9-methyladenine (9-MeAd) in solution of MeCN, PhCN, Me_3CCN and Ph_2(H)CCN. Reaction of **1a**,**b** and **2a**,**b** with HCl affords the protonated amidines [NH_2=C(R){1-MeCy(-H)}]NO_3 (R = Me, **3a**; Ph, **3b**) and [NH_2=C(R){9-MeAd(-H)}]NO_3 (R = Me, **4a**; Ph, **4b**) and *cis*-(PPh_3)$_2$$PtCl_2$ in quantitative yield. Treatment of **3b** and **4b** with NaOH allows the isolation of the neutral benzimidamides NH_2-C(Ph){1-MeCy(-2H)} (**5b**) and NH_2-C(Ph){9-MeAd(-2H)} (**6b**). In the solid state **3b** shows a planar structure with the hydrogen atom on N(4) cytosine position involved in a strong H-bond with the NO_3^- ion. Intermolecular H-bonds between the oxygen of the cytosine ring and one of the H atoms of the amidine-NH_2 group allow the dimerization of the molecule. A detailed analysis of the spectra of **3b** in DMF-d_7 at −55 °C indicates the presence of an equilibrium between the species [NH_2=C(R){1-MeCy(-H)}]NO_3 and [NH_2=C(R){1-MeCy(-H)}]$_2$(NO_3)$_2$, exchanging with trace amounts of water at 25 °C. [^{15}N,^{1}H]-HMBC experiments for **5b** and **6b** indicate that the *amino* tautomer H_2N-C(Ph){nucleobase(-2H)}, is the only detectable in solution and such structure has been confirmed in the solid state. The reaction of **5b** and **6b** with *cis*-$L_2Pt(ONO_2)_2$ (L = PPh_3), in chlorinated solvents, determines the immediate appearance of a pale yellow colour due to the coordination of the neutral amidine, likely in its *imino* form HN=C(Ph){nucleobase(-H)}, to give the adducts *cis*-[L_2PtNH=C(Ph){nucleobase(-H)}]$^{2+}$. In fact, addition of "proton sponge" leads to the immediate deprotonation of the amidine ligand with formation of the starting complexes **1b** and **2b**.

Introduction

Amidines, R–C(=NH)NH_2, their N-mono- and N,N′-disubstituted derivatives are important intermediates in the synthesis of heterocyclic compounds,[1] some of which are pharmacologically active molecules.[2] The usual synthetic methods proceed through: i) addition of metal amides to nitriles; ii) addition of salt of ammonia or amines to nitriles; iii) transformation of nitriles into imido esters followed by the condensation with NH_3 or amines (Pinner synthesis).[1,3] In several cases, the preparation needs high temperatures,[4] strongly reducing agents,[5] highly acidic or alkaline conditions.[6]

More recently, the activation of nitriles through coordination to a metal centre, increasing the rate of the nucleophilic attack at the carbon atom of the CN group,[7] led to the synthesis of several amidine complexes of transition metals, in particular of platinum(II and IV).[8] We have recently shown that, if the nucleophile is the nitrogen atom of the NH_2-deprotonated 1-methylcytosine (1-MeCy) and 9-methyladenine (9-MeAd) (Chart 1), the azametallacycle complexes of platinum(II) *cis*-[L_2PtNH=C(R){1-MeCy(-2H)}]$^+$ and *cis*-[L_2PtNH=C(R){9-MeAd(-2H)}]$^+$ (L = PPh_3 and $PMePh_2$) are formed.[9,10]

They contain as an anionic ligand the deprotonated form of the N-monosubstitute amidines R–C(=NH)NHR' (R = Me, Ph), in which the NHR' group is the nucleobase 1-MeCy or 9-MeAd, and are structurally similar to 1,3,5-triazapentadienes recently reviewed by Kopylovich and Pombeiro.[11]

In this paper we present the synthesis and the structural characterization of these new amidines, in their protonated and neutral forms, [NH_2=C(R){nucleobase(-H)}]NO_3, and NH_2-C(R){nucleobase(-2H)}, respectively. The ionic species are formed in high yield by protonation of the amidine complexes *cis*-[L_2PtNH=C(R){nucleobase(-2H)}]NO_3 (L = PPh_3; R = Me, Ph) with aqueous HCl, allowing the quantitative recovery of the

[a]*Dipartimento di Scienze Chimiche, Università di Padova, Via Marzolo 1, 35131, Padova, Italy. E-mail: diego.montagner@unipd.it; Fax: +39-049-8275161; Tel: +39-049-8275172*
[b]*Dipartimento di Scienze Chimiche e Farmaceutiche, Università di Trieste, Via Giorgieri 1, 34127, Trieste, Italy*
[c]*Dipartimento di Scienze Ambientali, Università Ca' Foscari di Venezia, Dorsoduro 2137, 30123, Venezia, Italy*

† Electronic supplementary information (ESI) available. CCDC reference numbers 811783–811786. For ESI and crystallographic data in CIF or other electronic format see DOI: 10.1039/c1dt10638d

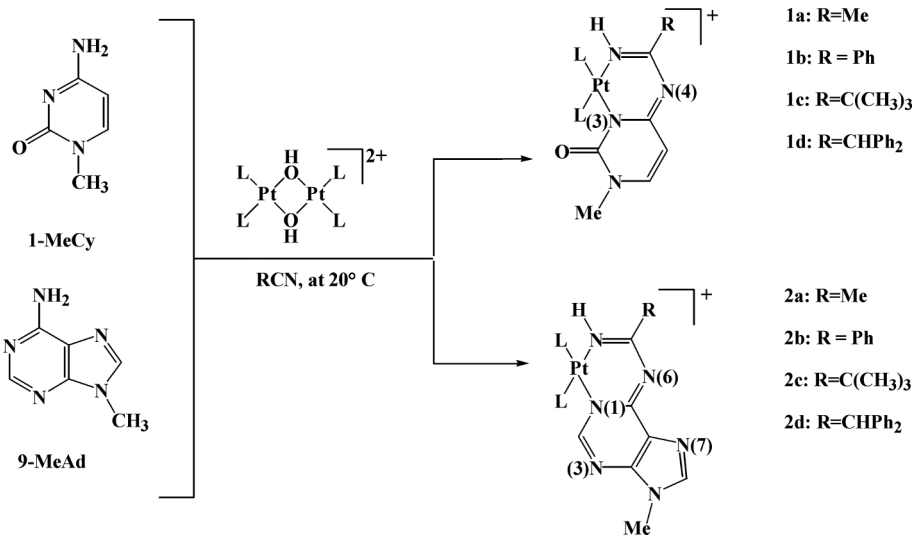

Chart 1 Synthetic procedures for the amidine Platinum(II) complexes (L = PPh_3, $PMePh_2$).

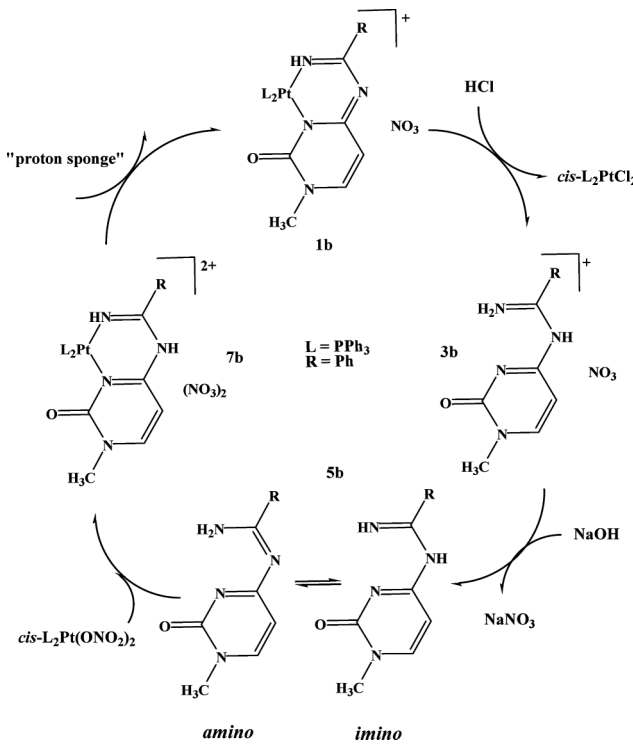

Chart 2 Synthetic pathway for the synthesis of amidines and their coordination properties.

metal as *cis*-$(PPh_3)_2PtCl_2$, as shown in Chart 2 for the 1-MeCy derivative.

The nitrato salt of *N*-(1-methyl-2-oxo-1,2-dihydropyrimidin-4-yl)benzimidamide, $[NH_2{=}C(Ph)\{1\text{-}MeCy(-H)\}]NO_3$, has been characterized by single crystal X-ray analysis and in solution by NMR at variable temperature. In the solid state, strong intermolecular H-bonds stabilize a dimeric structure of the cation, which is also maintained in solution of DMSO-d_6 or DMF-d_7.

The neutral species, of which the *amino* and the *imino* tautomeric forms are expected [NH_2-C(R){nucleobase(-2H)} and NH=C(R){nucleobase(-H)}, respectively] (Chart 2), have been obtained in the amino form, namely NH_2-C(Ph){1-MeCy(-2H)} and NH_2-C(Ph){9-MeAd(-2H)}, and this isomer is the preferred one, as confirmed by the structural characterization in the solid state and in solution. The stabilization of the *imino* tautomer through metal coordination has been also investigated by reacting these amidines with the complex *cis*-$L_2Pt(ONO_2)_2$ (L = PPh_3) containing the labile nitrato ligands.[12] The adducts, tentatively formulated as *cis*-$[L_2PtNH{=}C(Ph)\{nucleobase(-H)\}](NO_3)_2$, quantitatively convert into *cis*-$[L_2PtNH{=}C(Ph)\{nucleobase(-2H)\}]NO_3$, by addition of a "proton sponge".

The single crystal X-ray analysis of the cytosine derivative *cis*-$[(PPh_3)_2PtNH{=}C(Ph)\{1\text{-}MeCy(-2H)\}]NO_3$ confirms the coordination features of the anionic ligand previously described for the $PMePh_2$ analogue[10] and allows the examination of the structural differences between the free and the coordinated benzimidamides. Finally, the reactivity of Me_3C–CN and $Ph_2(H)C$–CN has been explored, showing that the insertion of these hindered nitriles into the platinum–nucleobase bond is incomplete in the case of 9-MeAd, while the amidine complexes *cis*-$[(PPh_3)_2PtNH{=}C(R)\{1\text{-}MeCy(-2H)\}]NO_3$ [R = Me_3C and $Ph_2(H)C$] can been isolated in high yield. They are structurally analogous to the acetonitrile and benzonitrile derivatives, suggesting that the use of appropriate nitriles can lead to a variety of metallacycle complexes from which new amidines can be prepared.

Experimental section

Instrumentation and materials

^1H, ^{13}C and ^{31}P NMR experiments were recorded on a Bruker AVANCE 300 MHz operating at 300.13, 121.49 and 100.61 MHZ, respectively. ^{15}N NMR with Bruker 400 AMX-WB spectrometer (operating at 40.6 MHz). The ^1H and ^{13}C chemical shifts were referenced to the residual impurity of the solvent and to TMS. The external references were H_3PO_4 (85% w/w in D_2O) for ^{31}P and CH_3NO_2 (in $CDCl_3$ at 50% w/w) for ^{15}N. Inverse detected spectra were obtained through heteronuclear multiple bond correlation

(HMBC) experiments, using parameters similar to those previously reported.[13]

IR spectra were recorded on a JASCO FT/IR-4100 type A Fourier Transform Infrared Spectrometer using Nujol mulls between KBr discs.

All the solvents (CH_2Cl_2, MeOH, PhCN, $CDCl_3$, D_2O, DMSO-d_6, DMF-d_7), HCl, NaOH, $Ph_2C(H)CN$, $(CH_3)_3CCN$ and $CH(OC_2H_5)_3$ are Aldrich products. 9-MeAd,[14] 1-MeCy,[15] *cis*-$[(PPh_3)_2Pt(\mu\text{-}OH)]_2(NO_3)_2$,[9] *cis*-$[(PPh_3)_2PtNH{=}C(R)\{1\text{-}MeCy(-2H)\}]NO_3$ (R = Me, **1a**; Ph, **1b**) and *cis*-$[(PPh_3)_2PtNH{=}C(Ph)\{9\text{-}MeAd(-2H)\}]NO_3$ (R = Me, **2a**; Ph, **2b**) were synthesized as previously reported.[9,10]

Synthetic work

1. *cis*-[(PPh$_3$)$_2$PtHN=C(CMe$_3$){1-MeCy(-2H)}]NO$_3$, 1c. A suspension of *cis*-$[(PPh_3)_2Pt(\mu\text{-}OH)]_2(NO_3)_2$ (32 mg, 2.0×10^{-2} mmol) and 1-MeCy (5.2 mg, 4.0×10^{-2} mmol) in $(CH_3)_3CCN$ (2 mL) and CH_2Cl_2 (4 mL) was stirred at r.t. for 24 h. Addition of Et_2O to the resulting yellow solution afforded the precipitation of a pale yellow solid, which was recovered by filtration, washed several times with Et_2O, and dried under vacuum. The yield of **1c** was 32 mg, 80%. Elemental analysis calcd (%) for $C_{46}H_{45}N_5O_4P_2Pt{\cdot}1/2CH_2Cl_2$: C 54.15, H 4.50, N 6.79; found C 54.62, H 4.66, N 7.02. ^{1}H NMR in $CDCl_3$ (δ, ppm): 7.50–7.21 (c.m., 30 H, Ph); 7.12 (d, $^3J_{HH}$ = 7.2 Hz, 1 H, H6); 6.03 (dd, $^3J_{HH}$ = 7.1 Hz, $^5J_{HP}$ = 1.5 Hz, 1 H, H5); 5.89 (br s, 1H, NH); 2.65 (s, 3 H, N(1)CH$_3$); 0.86 (s, 9H, CMe$_3$). ^{31}P{^{1}H} NMR in DMSO-d_6 (δ, ppm): 8.29 ($^1J_{PPt}$ = 3436 Hz); 8.01 ($^1J_{PPt}$ = 3479 Hz), $^2J_{PP}$ = 24.9 Hz. ^{1}H NMR in DMSO-d_6 (δ, ppm): 7.79–7.30 (c.m., 30 H, Ph); 7.27 (d, $^3J_{HH}$ = 7.4 Hz, 1H, H6); 5.92 (dd, $^3J_{HH}$ = 7.4 Hz, $^5J_{HP}$ = 1.0 Hz 1H, H5); 5.84 (br s, 1H, NH); 3.35 (s, 3 H, N(1)CH$_3$: 0.78 (s, 9H, CMe$_3$).

2. *cis*-[(PPh$_3$)$_2$PtHN=C(CHPh$_2$){1-MeCy(-2H)}]NO$_3$, 1d. A suspension of *cis*-$[(PPh_3)_2Pt(\mu\text{-}OH)]_2(NO_3)_2$ (502 mg, 3.1×10^{-1} mmol), 1-MeCy (79.2 mg, 6.3×10^{-1} mmol) and $Ph_2C(H)CN$ (128 mg, 6.6×10^{-1} mmol) in CH_2Cl_2 (5.0 mL) was stirred at *ca* 25 °C for 3 days. A trace amount of solid was eliminated by filtration and Et_2O (20 mL) was then added to the resulting yellow solution. The powdered precipitate was recovered by filtration, washed several times with Et_2O, and dried under vacuum, to give a yellow solid. The yield of **1d** was 585 mg, 92%. Elemental analysis calcd (%) for $C_{55}H_{47}N_5O_4P_2Pt{\cdot}CH_2Cl_2$: C 56.81, H 4.18, N 5.91; found C 56.49, H 4.21, N 6.09. ^{1}H NMR in $CDCl_3$ (δ, ppm): 7.62–6.68 (c.m., 41 H, Ph and H6); 6.07 (br s, 1H, NH; 5.93 (dd, $^3J_{HH}$ = 7.1 Hz, $^5J_{HP}$ = 1.2 Hz 1 H, H5); 5.18 (s, 1H, CH); 2.68 (s, 3H, N(1)CH$_3$. ^{31}P{^{1}H} NMR in DMSO-d_6 (δ, ppm): 7.71 ($^1J_{PPt}$ = 3523 Hz); 7.27 ($^1J_{PPt}$ = 3402 Hz), $^2J_{PP}$ = 25.3 Hz. ^{1}H NMR in DMSO-d_6 (δ, ppm): 7.75–6.75 (c.m., 41 H, Ph and H6); 6.28 (br s, 1H, NH); 5.86 (dd, $^3J_{HH}$ = 7.1 Hz, $^5J_{HP}$ = 1.2 Hz 1 H, H5); 5.28 (s, 1H, CH); 3.35 (s, 3H, N(1)CH$_3$).

3. [NH$_2$=C(Ph){1-MeCy(-H)}]NO$_3$, 3b. To a solution of **1b** (215 mg, 2.1×10^{-1} mmol) in CH_2Cl_2 (10 mL), a solution of HCl 0.05 M (8.53 mL, 4.3×10^{-1} mmol) was slowly added and the mixture let stirring for 2 h at r.t. The aqueous phase was then separated through a separating funnel and the solvent evaporated under vacuum at ambient temperature. The resulting white solid **3b** was 54.4 mg (yield 89%). Elemental analysis calcd (%) for **3b**; $C_{12}H_{13}N_5O_4$: C 49.48, H 4.51, N 24.03; found C 49.30, H 4.68, N 23.85. ^{1}H NMR in D_2O (δ, ppm): 8.13 (d, $^3J_{HH}$ = 7.1 Hz, 1H, H6); 7.81–7.59 (c.m., 5H, Ph); 6.50 (d, $^3J_{HH}$ = 7.1 Hz, 1H, H5); 3.53 (s, 3 H, N(1)CH$_3$). ^{13}C{^{1}H} NMR in D_2O (δ, ppm): 166.8 (C_{CN}); 158.3 (C2); 153.8 (C8); 135.0 (C_p); 130.2 (C_m); 129.3 (C_o); 128.1 (C_i); 99.2 (C5); 39.1 (NCH$_3$). ^{1}H NMR in DMSO-d_6 (δ, ppm): 12.12 (br s, 1H, NH); 11.87 (br s, 1H, NH); 9.81 (br s, 1H, NH); 8.26 (d, $^3J_{HH}$ = 7.5 Hz, 1H, H6); 7.97–7.88 (c.m., 5H, Ph); 6.48 (d, $^3J_{HH}$ = 7.5 Hz, 1H, H5); 3.44 (s, 3 H, N(1)CH$_3$). IR: ν_{NH} = 3458 and 3229 cm^{-1}; ν_{CO} = 1651 cm^{-1}. Suitable crystals for X-ray analysis were obtained from slow diffusion of Et_2O vapors into a MeOH solution of **3b**, at r.t. With the same procedure, **3a** was obtained starting from *cis*-$[(PPh_3)_2PtHN{=}C(Me)\{1\text{-}MeCy(-2H)\}]NO_3$. (yield 75%). Elemental analysis calcd (%) for **3a**; $C_7H_{11}N_5O_4$: C 36.68, H 4.85, N 30.54; found C 36.40, H 4.70, N 30.85. ^{1}H NMR in D_2O (δ, ppm): 8.13 (d, $^3J_{HH}$ = 7.05 Hz, 1H, H6); 6.40 (d, $^3J_{HH}$ = 7.05 Hz, 1H, H5); 3.57 (s, 3 H, N(1)CH$_3$); 2.48 (s, 3 H, CCH$_3$). ^{1}H NMR in DMSO-d_6 (δ, ppm): 11.22 (br s, 1H, NH); 11.12 (br s, 1H, NH); 11.08 (br s, 1H, NH); 8.24 (d, $^3J_{HH}$ = 6.51 Hz, 1H, H6); 6.22 (d, $^3J_{HH}$ = 6.51 Hz, 1H, H5); 3.51 (s, 3H, N(1)CH$_3$); 2.42 (s, 3H, CCH$_3$).

4. [NH$_2$=C(Ph){9-MeAd(-H)}]NO$_3$, 4b. With an analogue procedure, starting from **2b** (136 mg, 1.3×10^{-1} mmol), **4b** was prepared (55 mg, yield 89%). Elemental analysis calcd (%) for **4b**; $C_{13}H_{13}N_7O_3$: C 49.53, H 4.16, N 31.08; found C 49.32, H 4.34, N 31.25. ^{1}H NMR in D_2O (δ, ppm): 8.79 (s, 1H, H2); 8.36 (s, 1H, H8); 7.91–7.64 (c.m., 5H, Ph); 3.39 (s, 3H, N(9)CH$_3$). ^{13}C{^{1}H} NMR in D_2O (δ, ppm): 162.7 (C_{CN}); 159.7 (C2); 153.3 (C6); 151.3 (C4); 147.9 (C8); 135.4 (C5); 132.5 (C_p); 130.2 (C_m); 129.1 (C_o); 128.9 (C_i); 99.2 (C5); 30.9 (NCH$_3$). ^{1}H NMR in DMSO-d_6 (δ, ppm): 11.68 (br s, 1H, NH); 10.96 (br s, 2H, NH); 8.87 (s, 1H, H2); 8.68 (s, 1 H, H8); 7.91–7.77 (c.m., 5H, Ph); 3.90 (s, 3 H, N(9)CH$_3$). IR: ν_{NH} = 3453 and 3223 cm^{-1}. With the same procedure, **4a** was obtained starting from *cis*-$[(PPh_3)_2PtHN{=}C(Me)\{9\text{-}MeAd(-2H)\}]NO_3$. (yield 79%). Elemental analysis calcd (%) for **4a**; $C_8H_{11}N_7O_3$: C 37.95, H 4.39, N 38.71; found C 38.20, H 4.45, N 38.42. ^{1}H NMR in D_2O (δ, ppm): 8.77 (s, 1H, H2); 8.39 (s, 1H, H8); 3.93 (s, 3 H, N(1)CH$_3$); 2.61 (s, 3 H, CCH$_3$). ^{1}H NMR in DMSO-d_6 (δ, ppm): 11.56 (br s, 1H, NH); 10.94 (br s, 1H, NH); 8.70 (br s, 1H, NH); 8.94 (s, 1H, H2); 8.79 (s, 1H, H8); 3.87 (s, 3H, N(1)CH$_3$); 2.52 (s, 3 H, CCH$_3$).

5. H$_2$N-C(Ph){1-MeCy(-2H)}, 5b. To a solution of **3b** (120 mg, 4.1×10^{-1} mmol) in H_2O (4 mL) a solution of NaOH 0.1 M (4.1 mL) was added. The white precipitate that immediately formed was recovered by filtration, washed several times with H_2O and dried under vacuum. The yield of **5b** was 85%. Elemental analysis calcd (%) for **5b**; $C_{12}H_{12}N_4O$: C 63.15, H 5.31, N 24.53; found C 62.96, H 5.05, N 24.38. ^{1}H NMR in $CDCl_3$ (δ, ppm): 11.56 (br s, 1H, NH); 7.95–7.44 (c.m., 5H, Ph); 7.42 (d, $^3J_{HH}$ = 6.9 Hz, 1 H, H6); 7.14 (br s, 1H, NH); 6.25 (d, $^3J_{HH}$ = 6.9 Hz, 1 H, H5); 3.52 (s, 3 H, N(1)CH$_3$). ^{13}C{^{1}H} NMR in $CDCl_3$ (δ, ppm): 173.0 (C_{CN}); 165.1 (C4); 157.6 (C2); 146.0 (C6); 135.3 (C_p); 131.0 (C_m); 128.5 (C_o); 127.8 (C_i); 105.1 (C5); 38.3 (NCH$_3$). ^{1}H NMR in DMSO-d_6 (δ, ppm): 11.11 (br s, 1H, NH); 9.14 (br s, 1H, NH); 8.03–7.57 (c.m., 5H, Ph); 7.87 (d, $^3J_{HH}$ = 7.0 Hz, 1H, H6); 6.06 (d, $^3J_{HH}$ = 7.0 Hz, 1H, H5); 3.32 (s, 3 H, N(1)CH$_3$). IR: ν_{NH} = 3444 and 3183 cm^{-1}.

6. H_2N-C(Ph){9-MeAd(-2H)}, 6b. To a solution of **4b** (184 mg, 5.8×10^{-1} mmol) in H_2O (6 mL) a solution of NaOH 0.1 M (5.90 mL) was slowly added. The white precipitate immediately formed was recovered by filtration, washed with H_2O and dried under vacuum. The yield of **6b** was 97 mg, 66%. Elemental analysis calcd (%) for **6b**; $C_{13}H_{12}N_6$: C 61.90, H 4.80, N 33.30; found C 62.15, H 4.62, N 33.52. ^{1}H NMR in $CDCl_3$ (δ, ppm): 11.10 (br s, 1H, NH); 8.69 (s, 1H, H2); 8.11–7.45 (c.m., 6 H, Ph and H8); 5.95 (br s, 1H, NH); 3.89 (s, 3 H, N(9)CH_3). ^{13}C{^{1}H} NMR in $CDCl_3$ (δ, ppm): 163.4 (C_{CN}); 160.0 (C2); 152.7 (C6); 151.8 (C4); 143.5 (C8); 136.5 (C5); 132.4 (C_p); 129.3 (C_m); 128.7 (C_o); 128.4 (C_i); 30.6 (NCH_3). ^{1}H NMR in DMSO-d_6 (δ, ppm): 10.25 (br s, 1H, NH); 8.79 (br s, 1H, NH); 8.63 (s, 1H, H2); 8.28 (s, 1H, H8); 8.13–7.57 (c.m., 5 H, Ph); 3.79 (s, 3H, N(9)CH_3). IR: ν_{NH} = 3466 and 3252 cm^{-1}.

Suitable crystals for X-ray analyses of **5b** and **6b** were obtained from slow evaporation at r.t. of a solution in $CDCl_3$ into a NMR tube.

7. Relative stability of the amidine complexes. i) 18.5 mg of *cis*-[$(PPh_3)_2Pt(\mu$-OH)]$_2(NO_3)_2$ (1.2×10^{-2} mmol) and 1-MeCy (3.0 mg, 2.4×10^{-2} mmol) were rapidly dissolved in 0.8 mL of DMSO-d_6 solution containing equimolar amounts of Me_3CCN (39 mg), $Ph_2C(H)CN$ (93 mg) and CH_3CN (20 mg) in order to have Pt/each nitrile ratio 1/20. On the base of ^{31}P NMR spectra, immediately after the dissolution **1a**, **1c** and **1d** were in a ratio of 9 : 0 : 1, after 24 h the corresponding ratio was 7 : 1 : 2 and after 5 days at r.t. it became 2 : 1 : 7. ii) 21.2 mg of *cis*-[$(PPh_3)_2Pt(\mu$-OH)]$_2(NO_3)_2$ (1.3×10^{-2} mmol) and 1-MeCy (3.3 mg, 2.6×10^{-2} mmol) were dissolved in a mixture of 0.3 mL of CH_3CN and 0.3 mL of PhCN and the reaction was followed through ^{31}P NMR with D_2O as insert. Immediately after the dissolution the ratio between **1a**:**1b** was 3 : 2 but after 5 days at room temperature only **1b** was detectable.

X-ray structure determination

Crystal data and details of data collections and refinements for the structures reported are summarized in Table 1. Intensity data of compounds **1b**, **3b**, and **5b** were collected at room temperature (293(2) K) on a Nonius DIP-1030H system (Mo-Kα radiation, λ = 0.71073 Å), those of **6b** on a Nonius FR591 rotating anode (Cu-Kα, λ = 1.54178 Å), equipped with Kappa CCD imaging plate. Cell refinement, indexing and scaling for the data sets were performed by using Denzo and Scalepack programs.[16] All the structures were solved by direct methods and subsequent Fourier analyses[17] and refined by the full-matrix least-squares method based on F^2 with all observed reflections.[17] A molecule of diethylether was detected in the ΔF map of **1b**. Hydrogen atoms were positioned at geometrical calculated positions except those of amine group in **3b**, **5b**, and **6b**. All the calculations were performed using the WinGX System, Ver 1.80.05.[18]

Crystallographic data for this paper is available in the ESI, CCDC numbers 811783–811786.†

Results and discussion

Syntheses of the amidine complexes *cis*-[$(PPh_3)_2$PtNH=C(R)-{nucleobase(-2H)}]NO_3

We have recently shown that the dinuclear hydroxo complex *cis*-[$(PPh_3)_2Pt(\mu$-OH)]$_2(NO_3)_2$ reacts with 1-MeCy or 9-MeAd, in CH_3CN or PhCN, to give quantitatively the azametallacycles *cis*-[$(PPh_3)_2$PtNH=C(R){nucleobase(-2H)}]NO_3, as depicted in Chart 1. By monitoring the reaction with ^{31}P NMR, it was

Table 1 Crystal data and details of structure refinements for compounds **1b**, **3b**, **5b**, and **6b**

	1b·OEt_2	**3b**	**5b**	**6b**
Empirical formula	$C_{52}H_{51}N_5O_5P_2Pt$	$C_{12}H_{13}N_5O_4$	$C_{12}H_{12}N_4O$	$C_{13}H_{12}N_6$
Formula weight	1083.01	291.27	228.26	252.29
Crystal system	Triclinic	Monoclinic	Monoclinic	Triclinic
Space group	$P\bar{1}$	$P2_1/n$	$P2_1/n$	$P\bar{1}$
a (Å)	12.795(2)	10.426(2)	7.374(2)	10.681(2)
b (Å)	14.002(2)	9.226(2)	11.022(3)	10.645(3)
c (Å)	14.667(3)	14.336(3)	13.990(3)	12.011(3)
α (°)	114.857(9)			110.88(2)
β (°)	94.249(10)	94.01(2)	100.40(2)	91.87(2)
γ (°)	95.843(10)			95.54(2)
Volume (Å^3)	2351.9(7)	1375.6(5)	1118.4(5)	1266.7(5)
Z	2	4	4	4
D_c (g cm^{-3})	1.529	1.406	1.356	1.323
μ Mo-Kα, (mm^{-1})[b]	3.105	0.109	0.092	0.699
F(000)	1092	608	480	528
θ_{max} (°)	27.88	26.73	25.02	60.04
Reflns collected	34811	16205	8953	9412
Unique reflections	10835	2901	1874	3584
R_{int}	0.0550	0.0391	0.0887	0.0515
Observed $I > 2\sigma(I)$	8219	2134	795	1458
Parameters	587	200	161	357
Goodness of fit (F^2)	0.949	1.085	0.866	0.961
R_1 ($I > 2\sigma(I)$)[a]	0.0400	0.0621	0.0521	0.0507
wR_2[a]	0.0943	0.1920	0.1156	0.1238
Residuals (e/Å^3)	0.996, –0.541	0.412, –0.261	0.207, –0.164	0.132, –0.167

[a] $R1 = \Sigma \, ||Fo| - |Fc|| / \Sigma \, |Fo|$, $wR2 = [\Sigma \, w \, (Fo^2 - Fc^2)^2 / \Sigma w \, (Fo^2)^2]^{\frac{1}{2}}$ [b] μ Cu-Kα for **6b**.

shown that the formation of *cis*-[$(PPh_3)_2$PtNH=C(R){1-MeCy(-2H)}]NO_3 (R = Me, **1a**; Ph, **1b**) occurs at ambient temperature and no intermediates are detectable. In contrast, 9-MeAd undergoes deprotonation, giving initially the chelated-N^6,N^7 adeninate complex *cis*-[$(PPh_3)_2$Pt{9-MeAd(-H),N^6N^7}]NO_3,[19] which reacts with a solvent molecule only after several hours at room temperature, affording quantitatively the insertion products *cis*-[$(PPh_3)_2$PtNH=C(R){9-MeAd(-2H)}]NO_3, (R = Me, **2a**; Ph, **2b**).

A similar reaction pattern is observed when the deprotonation of 1-MeCy occurs in solution of CH_2Cl_2 in the presence of the substituted acetonitriles Me_3CCN or $Ph_2C(H)CN$ and the amidines *cis*-[$(PPh_3)_2$PtNH=C(R){1-MeCy(-2H)}]NO_3 [R = Me_3C, **1c**; $Ph_2(H)C$, **1d**] are formed in quantitative yield (by ^{31}P NMR). The products **1c** and **1d** have been isolated as pure compounds and characterized by multinuclear NMR spectroscopy in $CDCl_3$ and DMSO-d_6. In both the solvents, the compounds exhibit features similar to those of the CH_3CN and PhCN analogous (**1a** and **1b**), as shown in Table T1 (ESI†) where the ^{31}P and selected ^{1}H NMR in $CDCl_3$ data are collected. As previously observed for **1a**, complexes **1c** and **1d** in solution of DMSO-d_6 appear stable while in chlorinated solvents they slowly (a few days at 25 °C) decompose to give the free nitrile and uncharacterized platinum complexes. The reaction is reversible as indicated by the immediate and quantitative formation of the amidine complexes **1c** and **1d** upon addition of an excess of Me_3CCN or $Ph_2C(H)CN$, respectively. The relative thermodynamic stability of the amidinic complexes **1a–1b** was investigated by reacting the hydroxo complex and 1-MeCy in mixture of CH_3CN and PhCN (see experimental). **1a** and **1b** are rapidly formed in a molar ratio *ca.* 3 : 2 and the composition of the reaction mixture slowly changed, leading to the quantitative presence of **1b** in few days at r.t. The effect of the stabilization due to the presence of phenyl rings in the nitrile molecule is confirmed in another experiment where it has been observed that, carrying out the condensation reaction in DMSO-d_6 with an equimolar mixture of CH_3CN, Me_3CCN and $Ph_2C(H)CN$, the relative concentration of **1a**, **1c** and **1d**, at the equilibrium (after 5 days at 25 °C) was 2 : 1 : 7.

As previously seen for CH_3CN and PhCN,[9,10] the reaction of *cis*-[$(PPh_3)_2$Pt(μ-OH)]$_2(NO_3)_2$ with 9-MeAd in CH_2Cl_2, in the presence of an excess of Me_3CCN or $Ph_2C(H)CN$, rapidly affords the intermediate *cis*-[$(PPh_3)_2$Pt{9-MeAd(-H),N^6N^7}]$^+$,[19] which slowly reacts with the nitrile to give the amidines *cis*-[$(PPh_3)_2$PtNH=C(R){9-MeAd(-2H)}]NO_3 (R = Me_3C, **2c**; $Ph_2(H)C$, **2d**). However the insertion of the nitrile molecule into the Pt-N(6) bond is not quantitative, even in the presence of a large excess of nitrile. As an example, the ^{31}P NMR spectrum of a mixture of *cis*-[$(PPh_3)_2$Pt(μ-OH)]$_2(NO_3)_2$, 9-MeAd and $Ph_2C(H)CN$, in molar ratio 1 : 2 : 20, is shown in Fig. S1 (ESI†). The AB pattern detected in the fresh prepared solution (Fig. S1a, ESI†), at δ 8.78 ($^1J_{PPt}$ = 3860 Hz) and 6.16 ppm ($^1J_{PPt}$ = 3100 Hz; $^2J_{PP}$ = 20 Hz), is attributable to the N^6,N^7-chelated adeninate complex, and its relative concentration is about 40% after 8 days (Fig. S1b, ESI†). These results reflect the relatively high thermodynamic stability of the five membered *N6*,*N7*-chelated adenine complex with respect to the amidine derivative **2d**. Although **2c** and **2d** were not isolated as pure compounds, their ^{31}P NMR in $CDCl_3$ parameters are included in Table T1 (ESI†). The chemical shift and coupling constant values for these compounds also suggest a structure similar to those of **2a** and **2b**, previously characterized.[9,10]

Syntheses and characterization of the amidines [NH_2=C(R)-{nucleobase(-H)}]NO_3 and NH_2-C(R){nucleobase(-2H)}

Addition of two equivalents of aqueous HCl to CH_2Cl_2 solutions of **1a**,**b** and **2a**,**b** leads to the immediate and quantitative protonation of the amidine ligands, released as nitrate salts [NH_2=C(R){nucleobase(-H)}]NO_3 (nucleobase: 1-MeCy, R = Me, **3a**; Ph, **3b**; 9-MeAd, R = Me, **4a**; Ph, **4b**), and the concomitant coordination of the chloride ions to the metal centre (Chart 2). The platinum containing product, *cis*-$(PPh_3)_2PtCl_2$, dissolved in the chlorinated solvent, can be quantitatively separated from the reaction mixture.

All these organic compounds are insoluble in chlorinated solvents whereas they easily dissolve in H_2O, DMSO and DMF. Compounds **3a** and **4a**, unlike the benzonitrile derivatives **3b** and **4b**, slowly decompose in water (a few days, at room temperature) with formation of CH_3CN and of the protonated nucleobases [1-MeCyH]NO_3 and [9-MeAdH]NO_3. Therefore, only **3b** and **4b** have been further characterized as neutral species, according to Chart 2.

Aqueous solutions of **3b** and **4b**, upon addition of stoichiometric amounts of NaOH, afford white precipitates of the neutral amidines NH_2-C(Ph){1-MeCy(-2H)} (**5b**) and NH_2-C(Ph){9-MeAd(-2H)} (**6b**) which have been characterized in solution by multinuclear NMR spectroscopy and in the solid state by single crystal X-ray analysis. These neutral species, insoluble in H_2O, dissolve in $CDCl_3$ and DMSO-d_6, where they appear indefinitely stable. The ^{1}H NMR spectra of **5b** and **6b** exhibit well-resolved doublets for the cytosine H5 and H6 protons and very sharp singlets for H2 and H8 adenine signals. The NH resonances are observed as two broad singlets having the same relative intensities, with very different chemical shift values ($\Delta\delta$ 4.4 and 5.1 ppm for **5b** and **6b**, respectively, in $CDCl_3$). ^{1}H,^{15}N HMQC experiments (Fig. S2, ESI†) of **5b** indicate that both the NH signals at δ 11.56 and 7.14 ppm correlate with the same ^{15}N nucleus (at δ −266 ppm), in agreement with the presence of two hydrogen atoms bound to the same nitrogen. Of the two possible tautomers of these amidines (Chart 2), the *amino* form appears to be the only one detectable in solution, as predicted by Prevorsek.[20] The large chemical shift difference for the NH_2 protons can be accounted for by the presence of relatively strong *intermolecular* hydrogen bonds, as detected in the solid state structure of **5b** and **6b** and discussed in the next section (Fig. S3 and S4, ESI†).

A more complex ^{1}H NMR pattern was observed in the case of the protonated amidine **3b**. In fact, whereas in D_2O the endocyclic protons H(6) and H(5) are observed as sharp doublets, with $^3J_{HH}$ = 7.07 Hz, they occur as poorly resolved doublets in DMSO-d_6. This unprecedented behaviour prompted us to study the system in DMF-d_7 at variable temperature. In this medium, at 25 °C, H5 and H6 show very broad singlets at 7.4 and 9.0 ppm, respectively, and a sharp singlet at 3.57 ppm for the N(1) methyl group. The NH proton resonances, undetectable in D_2O, are observed as very broad singlets, with the same relative intensities, at 13.4, 12.9 and 12.6 ppm in DMF-d_7. Decreasing the temperature to −55 °C, a sharpening of all the NH resonances is observed, with the concomitant progressive merging of those at higher field, to give a single resonance at 13.8 ppm, as shown in Fig. 1. A similar trend with the temperature is observed for

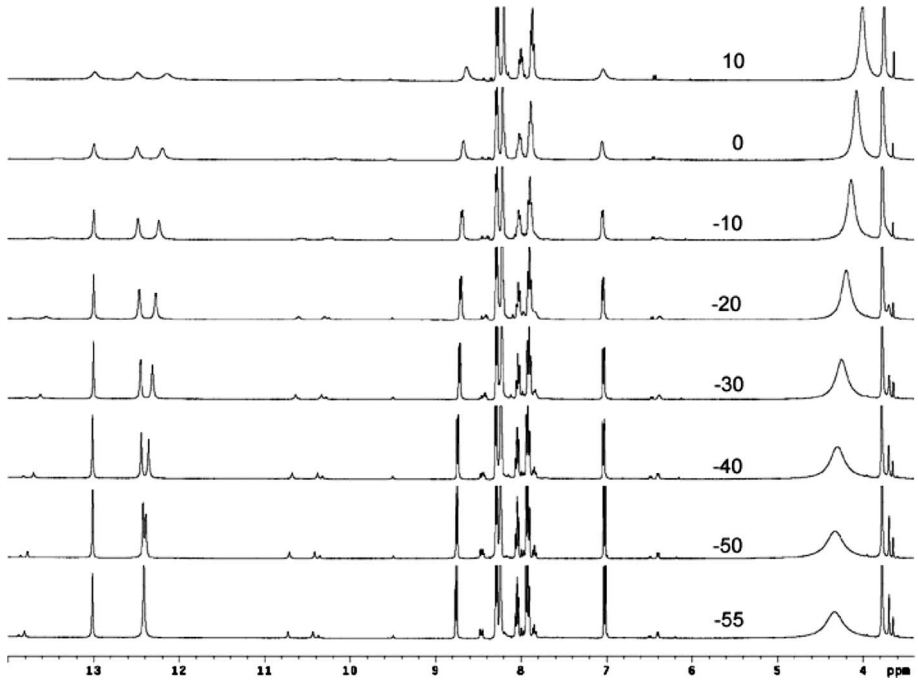

Fig. 1 Temperature dependence of the equilibrium between the monomer **3b** and the dimer **3b′** in DMF-d_7. Only selected temperatures are shown.

the H5 and H6 signals, which become sharp doublets at low temperature.

NMR investigation of the H-bonded monomer–dimer equilibrium of 3b

Inspection of Fig. 5 reveals in **3b** the presence of dimeric species formed *via* H-bonding between the iminium protons at N2 and the carbonylic oxygen O2. In addition, the aminic proton N4 and one nitrate oxygen are at H-bonding distance. These features are almost exactly reproduced in solution of DMF-d_7, as revealed by the ^{1}H NMR spectra monitored at different temperatures (Fig. 1). The dynamic behaviour in solution discloses other relevant features.

In the ^{1}H NMR spectrum recorded at −50 °C, three major broad peaks are observed between 12.2 and 13.2 ppm, *i.e.* within the typical H-bonding resonance range, beside three minor peaks: one in the H-bonding resonance range (δ = 13.8 ppm), the last two are somehow more shielded (δ = 10.75 and 10.42 ppm). These are NH resonances which can be accounted for due to the dimer–monomer equilibrium illustrated in Chart 3.

On the basis of this scheme, two major resonances, in the H-bond region and assigned to the NH protons of the iminium moiety, account for the formation of the dimer **3b′**. The minor resonances in the more shielded region are again the NH resonances of the iminium moiety in the "free" monomer **3b**, and the last major and minor resonances in the H-bond region pertain to the aminic proton of the dimer and of the monomer, respectively, that are H-bonded to the nitrate anion. The presence of H-bonds in solution between aminic protons and inorganic anions is documented.[21] This case is somehow different from the picture given by the X-ray diffraction analysis reported in Fig. 5, which highlights the presence of a dimer **3b″** with only two different H-bond interactions: of the aminic proton with the nitrate anion, and of only one iminium proton with carbonylic oxygen. This may be a situation dictated by packing requirements of the crystalline state.

The presence of the three major resonances in the H-bond region may be accounted for due to the dimeric structure of **3b′**. Alternatively, the equilibrium, fast at room temperature, between the dimeric strucure **3b″** and **3b‴** can be proposed. However, this situation would lead to an averaged NH resonance in a more shielded region. Thus the arrangement **3b′** that is to be preferred, would require the slow proton exchange between water (always present) and the aminium an iminium centers, and also the low rotation around the CN double bond.

At higher temperatures, the increasing exchange rates for the monomer–dimer equilibrium bring about the broadening and the final collapse of the NH resonances present in equivalent positions. This dynamic behaviour can be monitored and quantified in terms of equilibrium constants (see below) up to about 0 °C; at higher temperatures contaminations by other phenomena (rotations and proton exchanges) will interfere.

The thermodynamic behaviour can be monitored from other resonances of the monomer-dimer system, which therefore must be exactly attributed. Proton 5 and 6 of the 2-oxopyrimidine ring are in the form of doublets, in both structures, and therefore easily recognized, but not singularly assigned. The attribution procedure occurs *via* a NOESY experiment that at −55 °C is ambiguous: both the monomer and the dimer are in the "negative" NOE region, and the dipolar interactions are indistinguishable from exchange interactions. At 20 °C the resonances of the 2-oxopyrimidine ring collapse into two broad singlets. In the NOESY spectrum in Fig. S5 (ESI†), the deshielded singlet at 8.60 ppm belonging to proton 6 gives dipolar interaction with the methyl signal at 3.75 ppm. The shielded singlet at 7.02 ppm gives a dipolar interaction with the

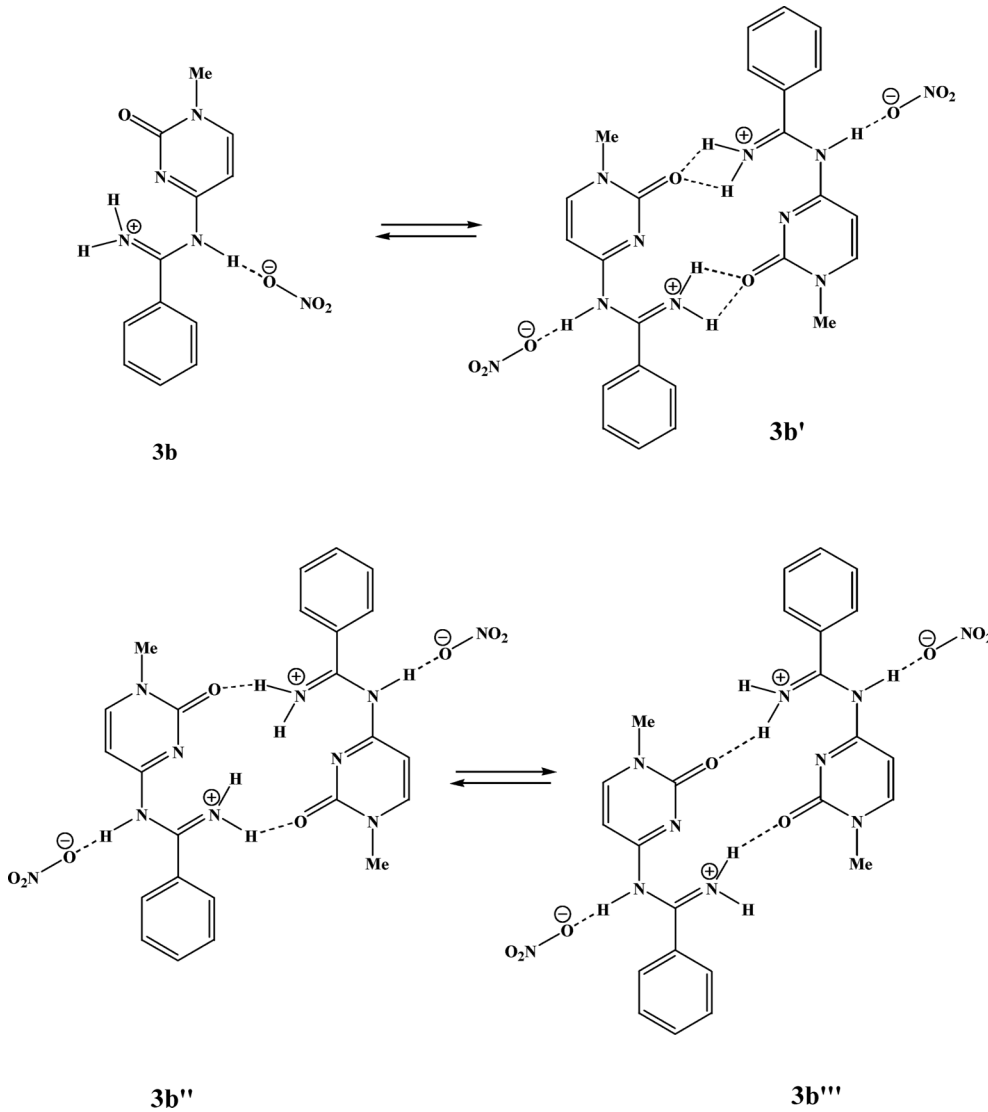

Chart 3 Dimer–monomer equilibrium of **3b**.

intense water signal at 3.95 ppm, denouncing the proximity to the aminic proton (which exchanges fast with water protons): this is the signal of proton 5 (See Fig. S5, ESI†).

At low temperatures, the resonances of protons 5 and 6 split into two pairs of doublets. The doublets of protons 6 resonate in a free region and will be utilized for a quantitative evaluation of the thermodynamics *via* the van'Hoff analysis of the monomer–dimer interconversion.

Van't Hoff plot

The integration of NMR peaks is, among the NMR parameters, the one measured with the least accuracy, also because of the limits of the instrumental numeric procedure. We therefore adopted the strategy of fitting the peaks into a combination of Gaussian and Lorentzian functions, followed by the analytical integration of these. The fitting is computationally accomplished with the Levenberg–Marquardt method.[22] Accurate integration values can be acquired between −55 and 15 °C, *i.e.* just below the coalescence temperature. The equilibrium constant K for the process is defined by:

$$2\ \text{monomer}\ \mathbf{3b} \underset{\text{Kdm}}{\overset{\text{Kmd}}{\rightleftharpoons}} \text{dimer}\ \mathbf{3b'}$$

where $K = \dfrac{[\text{dimer } \mathbf{3b'}]}{[\text{monomer } \mathbf{3b}]^2}$ and 2 [dimer **3b′**] + [monomer **3b**] = 0.011 mol L^{-1}

This is a non-equimolar equilibrium, and therefore the concentration of **3b** in DMF-d_7 must be determined with utmost accuracy, more for a correct evaluation of the equilibrium entropy $\Delta S°$ than for the evaluation of the equilibrium enthalpy $\Delta H°$. The monomer **3b** and DMF-d_7 were weighed in the NMR tube, and the concentration was checked after the measurement session by the further addition of a weighed amount of a substance with relevant molecular weight and one small 1H peak resonating in a free region: the choice was triethyl orthoformate.

From the Van't Hoff plot, the thermodynamic parameters $\Delta H°$ = −1.58 kcal L mol^{-1} and $\Delta S°$ = 9.01 cal K^{-1} L mol^{-1} are determined.

The positive entropy change for a dimerization process is unexpected so we then verified the accuracy of the results with the analytical integration of other signals, the NH and the methyl resonances, retrieving very similar positive values. Some comments on this point are necessary. Positive entropy changes for dimerization processes promoted by intermolecular H-bonding are not common, and are invariably associated with condensed phase experiments run in highly polar solvents.[23] A rationalization has been offered.[24] Since the molecular dipole vectors of two molecules such as **3b** mutually cancel upon the formation of a H-bonded dimer, the latter species possesses no molecular dipole vector. Highly polar solvent molecules are heavily organized around the monomer with relevant dipole vector, but to a relevantly minor extent around a dimer lacking a molecular dipole vector.

X-ray structural studies

The X-ray structural determination of complex **1b** shows the insertion of the benzonitrile molecule into the cytosine Pt-N(4) bond with formation of a six-membered ring, as depicted in Fig. 2. Selected bond distances and angles are collected in Table 2.

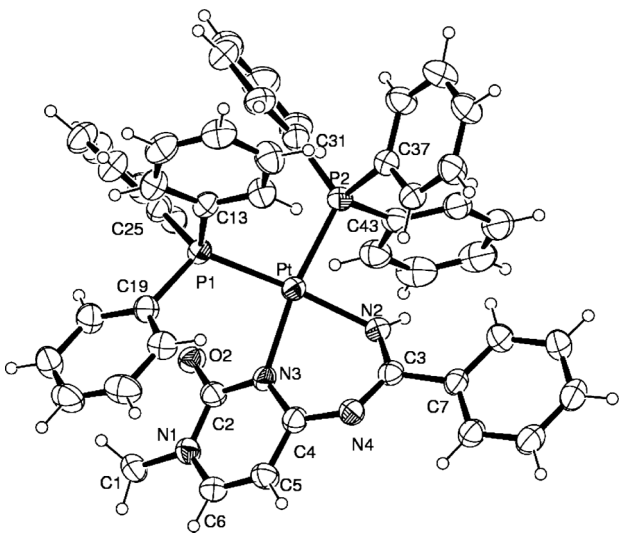

Fig. 2 ORTEP drawing (35% probability ellipsoids) of the cation of **1b**.

The platinum is bound to the nucleobase donor site N3, the inserted benzonitrile nitrogen N2, and completes the square planar coordination through phosphorus donors. The Pt–N3 and Pt–N2 bond distances are of 2.074(4) and 2.052(4) Å. The former bond length appears slightly shorter, the other longer with respect to the values measured in complexes *cis*-[$(PMePh_2)_2$PtNH=C(R){1-MeCy(-2H)}]$^+$ with R = Me[9] (2.097(4) and 2.036(4) Å, respectively) and Ph[10] (2.112(7) and 2.043(6) Å). The Pt–P bond distances are 2.2955(12) and 2.2898(13) Å. The N_2P_2 donors show a slight tetrahedral distortion in **1b**, with deviations up to ±0.22 Å from their mean plane. The amidine fragment results bowed with the cytosine and phenyl from the benzonitrile that formed an angle of 15.0(1)°, while the nucleobase ring forms a dihedral angle of 49.2(1)° with the mean coordination plane N_2P_2. Inside the six-membered ring fragment, the geometrical parameters indicate an electron delocalization. The molecule shows a π–π stacking between the cytosine and PPh_3 phenyl ring C(19) and a slightly stronger interaction between the phenyl rings C(25) and C(31) of the two PPh_3 (distance between ring centroids of 3.69 and 3.47 Å, dihedral angle 20.34 and 8.38°, respectively).

Table 2 Selected bond lengths (Å) and angles (°) of **1b**

Pt–N(2)	2.052(4)	Pt–P(1)	2.2955(12)
Pt–N(3)	2.074(4)	Pt–P(2)	2.2898(13)
N(2)–Pt–N(3)	82.20(14)	N(3)–Pt–P(1)	92.35(10)
N(2)–Pt–P(1)	165.21(12)	N(3)–Pt–P(2)	166.67(11)
N(2)–Pt–P(2)	88.48(11)	P(2)–Pt–P(1)	98.92(5)

The molecular structures of the protonated and neutral benzimidamide [NH_2=C(Ph){1-MeCy(-H)}]NO_3 (**3b**) and NH_2-C(Ph){1-MeCy(-2H)} (**5b**) are depicted in Figs. 3 and 4 respectively. The

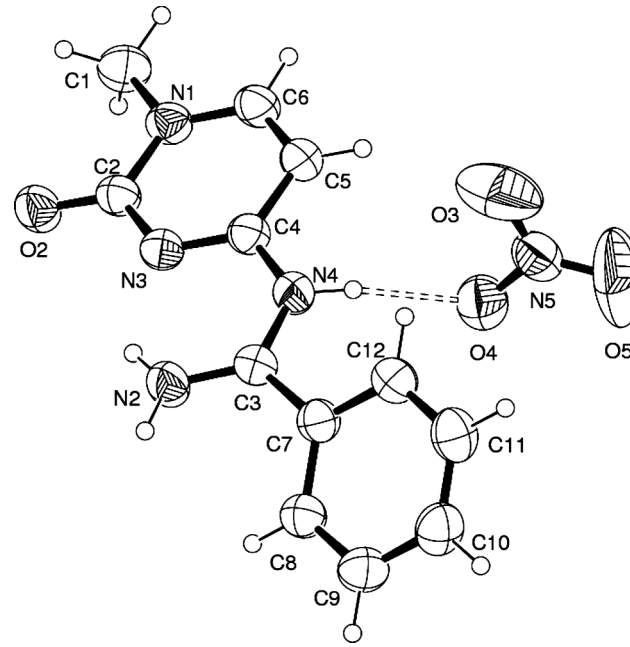

Fig. 3 ORTEP drawing (35% probability ellipsoids) of compound **3b**.

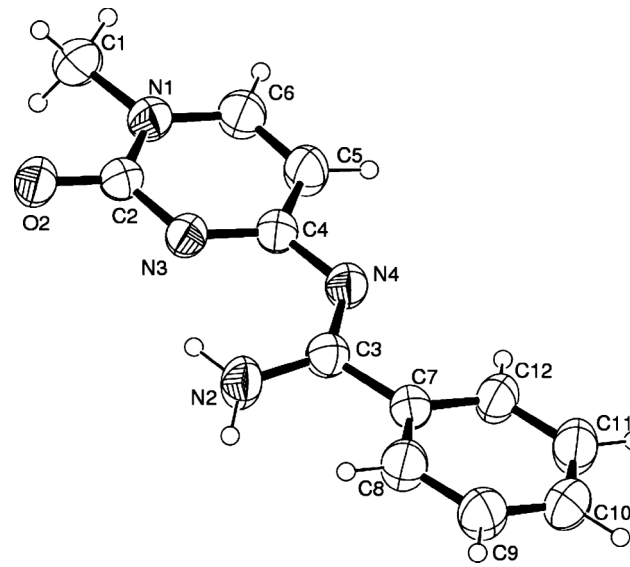

Fig. 4 ORTEP drawing (35% probability ellipsoids) of compound **5b**.

Table 3 Comparison of bond lengths (Å) and angles (°) of the amidine fragment in complexes *cis*-[(PMePh$_2$)$_2$PtNH═C(Me){1-MeCy(-2H)}]NO$_3$ (*5a* in ref [9]), *cis*-[(PMePh$_2$)$_2$PtNH═C(Ph){1-MeCy(-2H)}]NO$_3$ (*2* ref [10]), **1b** and in the free ligands **3b** and **5b**

	5a ref [9]	*2* ref [10]	**1b**	**3b**	**5b**
N(3)–C(4)	1.358(7)	1.339(10)	1.347(6)	1.306(3)	1.329(4)
C(4)–N(4)	1.356(7)	1.342(10)	1.351(6)	1.399(3)	1.372(4)
N(4)–C(3)	1.337(7)	1.302(10)	1.342(6)	1.361(3)	1.316(4)
C(3)–N(2)	1.295(7)	1.327(10)	1.312(6)	1.291(3)	1.325(4)
C(3)–C(7)	1.503(8)	1.488(10)	1.507(6)	1.472(3)	1.482(4)
C(3)–N(4)–C(4)	122.6(5)	122.8(8)	121.1(4)	127.54(17)	122.8(3)
N(3)–C(4)–N(4)	125.6(5)	127.5(9)	124.9(5)	119.14(17)	122.8(3)
N(4)–C(3)–N(2)	126.7(5)	126.7(8)	126.6(4)	121.46(19)	125.5(3)

geometrical parameters of the amidine moiety for these species are reported in Table 3 together with the corresponding values measured in complexes **1b** and *cis*-[(PMePh$_2$)$_2$PtNH═C(R){1-MeCy(-2H)}]$^+$ (R = Me[9] and Ph[10]). The protonated amidine **3b** shows the most striking differences: in particular in the fragment N(2)–C(3)–N(4)–C(4) where the former bond distance is shorter (1.291(3) Å) and the other longer (1.361(3), 1.399(3) Å, respectively) with regard to the values found in the metal complexes and in **5b**. Correspondingly, the angle C(3)–N(4)–C(4) of 127.54(17)° is the largest among those reported for the presence of the proton on N(4) which acts as a H donor towards the nitrate. In addition, the bond angles N(3)–C(4)–N(4) appear narrower (119.14(17) and 122.8(3)° in **3b** and **5b**, respectively, than the values observed in the complexes. The phenyl ring is tilted by 29.86(5) and 7.1(2)° in amidine molecules **3b** and **5b**, respectively. A more interesting observation is that the dihedral angle formed by the cytosine ring with the C7/C3/N2/N4 moiety, of *ca.* 9° in both, while upon coordination the measured value observed in **1b** is 25.7(1)°. In the crystal the molecular cations of **3b** are paired through H-bond interactions, beside the N4–H···O2 interaction cited above (Fig. 5)

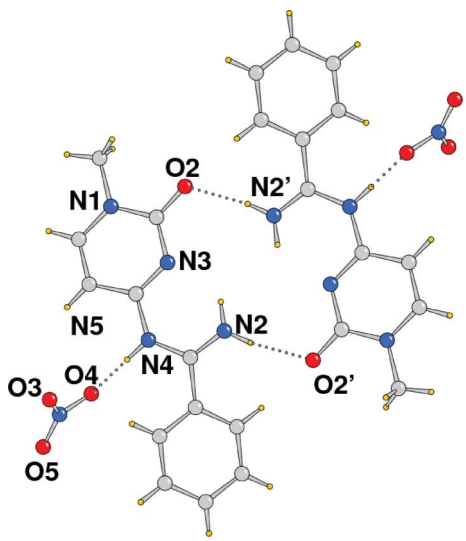

Fig. 5 Crystal packing of **3b** showing the dimers formed through H-bond interactions, (primed atoms at 2–x, 1–y, 1–z).

The structural analysis of **6b** shows the presence in the unit cell of two independent molecules (Fig. 6) which are very similar as far as their geometry is concerned. These molecules form a

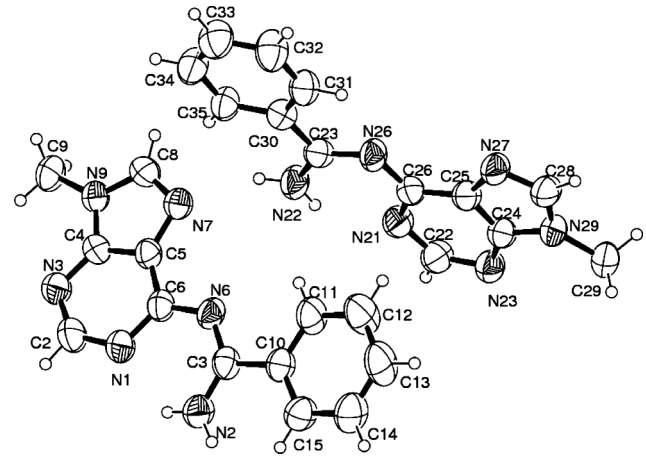

Fig. 6 ORTEP drawing (35% probability ellipsoids) of the two independent molecules of **6b**.

polymeric arrangement being alternatively connected along axis *b* by H bonds involving the amino group N2 and the endocyclic nitrogen N7 of the adjacent adenine moiety (N···N distance of *ca.* 2.97 Å), as depicted in Fig. S3 (ESI†). In Table T2 (ESI†) we report a comparison of the geometrical parameters of the two molecules A and B with the data obtained from the Pt complex **2b** and of complexes containing the amidine ligand derived from the acetonitrile.

These data clearly show a shortening of the C(3)–N(2) bond distance upon coordination (range 1.279(11)–1.295(8) Å *vs.* 1.324(5) and 1.334(4) Å in the free amidines), with a concurrent widening of the N(1)–C(6)–N(6) angle (mean values of 127.4° *vs.* 123.3°, respectively). Moreover the C(6)–N(6) bond distances in the free molecules A and B appear elongated with respect to the value measured upon coordination.

Here, and in the corresponding analysis of the amidine ligand built from the cystosine base (Table 3), it is not straightforward to derive a clear trend between the free and the coordinated species. Making allowance for e.s.d.'s of the geometrical data, this may be ascribed to the electron delocalization in the molecules, to the H-bonding scheme observed among the free benzimidamides in the solid state, but also to the deformations assumed by the chelating amidine–nucleobase fragment in the complex (likely to accomplish steric requirements) with respect to the planar arrangement found in the free molecules.

Coordination properties of the neutral amidines NH$_2$-C(Ph)-{nucleobase(-2H)}

The data so far reported for the neutral amidines **5b** and **6b** clearly support the presence in the solid and in solution of the *amino* tautomer (Chart 2). The stabilization of the *imino* form likely occurs when these molecules react with the complex *cis*-(PPh$_3$)$_2$Pt(ONO$_2$)$_2$.[12] In fact, addition of stoichiometric amounts of **5b** or **6b** to a colourless solution of the nitrato complex causes the immediate appearance of a pale yellow colour attributable to the replacement of the nitrato ligands in the coordination sphere of the metal and the concomitant formation of the adducts *cis*-[(PPh$_3$)$_2$PtNH═C(Ph){nucleobase(-H)}]$^{2+}$, depicted in Chart 2 for the NH═C(Ph){1-MeCy(-H)} derivative. Thus, the reaction of **5b** with *cis*-(PPh$_3$)$_2$Pt(ONO$_2$)$_2$, in CDCl$_3$, causes the immediate

change of the ^{31}P NMR spectrum, shown in Fig. 7, in which the singlet at δ 3.50 ($^{1}J_{PPt}$ = 4018 Hz) of the nitrato complex is completely replaced by an AB multiplet at 4.80 ($^{1}J_{PPt}$ = 3504 Hz) and 6.58 ppm ($^{1}J_{PPt}$ = 3543; $^{2}J_{PP}$ = 25.1 Hz), attributable to the adduct *cis*-[$(PPh_3)_2$PtNH=C(Ph){1-MeCy(-H)}]$^{2+}$ (**7b**). The values of coupling constants ^{31}P–^{195}Pt, slightly increased (an average of 72 Hz) with respect to those of the strictly related species *cis*-[$(PPh_3)_2$PtNH=C(Ph){1-MeCy(-2H)}]$^{+}$ (**1b**), strongly support the presence in **7** of the neutral amidine acting as a *N*,*N*-chelating ligand.

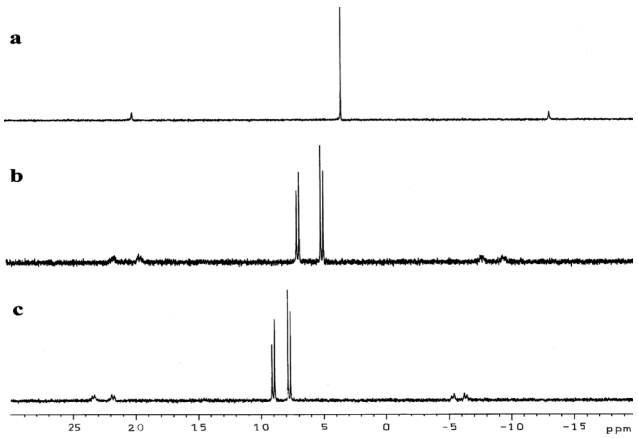

Fig. 7 $^{31}P\{^{1}H\}$NMR spectra in $CDCl_3$ of: a) *cis*-$(PPh_3)_2Pt(ONO_2)_2$; b) after addition of NH_2-C(Ph) {1-MeCy(-2H)}, **5b**; *c*) after addition of "proton sponge".

Moreover, addition of "proton sponge" to the $CDCl_3$ solution of **7b** causes the immediate deprotonation of the *imino* ligand, with the quantitative formation of complex **1b**, as shown in Fig. 7c. In the same experimental conditions, a more complex ^{31}P NMR spectrum was observed when **6b** was reacted with *cis*-$(PPh_3)_2Pt(ONO_2)_2$. In addition to the strong AB pattern at 7.73 ($^{1}J_{PPt}$ = 3467 Hz) and 8.01 ppm ($^{1}J_{PPt}$ = 3413; $^{2}J_{PP}$ = 24.5 Hz), attributed to the adduct *cis*-[$(PPh_3)_2$Pt NH=C(Ph){9-MeAd(-H)}]$^{2+}$ (**8b**), several weak signals in the range 4–16 ppm were also detected. However, addition of a "proton sponge" caused the immediate disappearance of all these signals, quantitatively replaced by those of the AB multiplet of *cis*-[$(PPh_3)_2$Pt NH=C(Ph){9-MeAd(-2H)}]$^{+}$, **2b**. We are currently trying to crystallize complexes **7b** and **8b** for a complete characterization in solution and in the solid state. It is interesting to note that the related species **2a**,**b** together with the analogs **1a**,**b** exhibit interesting cytotoxic properties toward several human tumour cell lines.[25]

Conclusions

The synthesis and structural characterization of the substituted amidines (*Z*)-*N*-(1-methyl-2-oxo-1,2-dihydropyramidin-4-yl)benzimidamide (**5b**) and (*Z*)-*N*′-(9-methyl-9*H*-purin-6-yl)benzimidamide (**6b**) and their nitrato salts **3b** and **4b**, are described. The compounds are formed by protonation with HCl of the metallacycles *cis*-[$(PPh_3)_2$PtNH=C(Ph){nucleobase(-2H)}]$^{+}$, which are quantitatively obtained by formal insertion of a molecule of PhCN molecule into the Pt–N(4) or Pt–N(6) bond of a platinum–cytosine or adenine complex, respectively. The high affinity of the chloride ions toward the Pt(II) centre, with formation of *cis*-$(PPh_3)_2PtCl_2$, allows the quantitative recovery of the metal. The planar structure of **3b** in the solid state is stabilized by a strong H-bond between the NO_3^- ion and the hydrogen atom on N(4) cytosine, whereas *intermolecular* H-bonds between the oxygen of the cytosine ring and one of the H atoms of the amidine-NH_2 group lead to the dimerization of the molecule. The analysis of the proton spectrum of **3b** in DMF-d_7 shows the presence of an equilibrium between the monomer and the dimer, both exchanging with trace amounts of water, at room temperature.

In addition to MeCN and PhCN, the nucleophylic attack of the NH_2-deprotonated nucleobase occurs to the metal-activated nitriles Me_3CCN and $Ph_2C(H)CN$ to give the amidine complexes *cis*-[$(PPh_3)_2$PtNH=C(R){nucleobase(-2H)}]NO_3, isolated in high yield for the 1-methylcytosine derivative. The method of synthesis here reported for the benzimidamides **5a** and **6b** can therefore be applied for the preparation of new amidines of type RC(=NH)NHR where the NHR fragment is the model nucleobase 1-methylcytosine or 9-methyladenine,

Acknowledgements

Dr D. Montagner thanks the University of Padua for the postdoc fellowship.

References

1 J. A. Gautier, M. Miocque and C. C. Farnoux, in *The Chemistry of Amidines and Imidates*, Vol. 1 (Ed., S. Patai), John Wiley, New York, 1975, pp. 283–348; G. V. Boyd, in *The Chemistry of Amidines and Imidates*, Vol. 2 (ed. S. Patai and Z. Rappoport), John Wiley, New York, 1991, pp. 367–424.
2 J. V. Greenhill and P. Lue, *Prog. Med. Chem.*, 1993, **30**, 203–326.
3 F. C. Schäfer and A. P. Krapcho, *J. Org. Chem.*, 1962, **27**, 1255–1258.
4 M. W. Partridge and W. F. Short, *J. Org. Chem.*, 1947, 390–394.
5 H. Jendralla, B. Seuring, J. Herchen, B. Kulitzscher, J. Wunner, W. Stuber and R. Koschinsky, *Tetrahedron*, 1995, **51**, 12047–12068; A. Dondoni and G. Barbaro, *J. Chem. Soc., Chem. Commun.*, 1975, 761–762; R. E. Bolton, S. J. Coote, H. Finch, A. Lowdon, N. Pegg and M. V. Vinader, *Tetrahedron Lett.*, 1995, **36**, 4471–4474.
6 H. U. Stilz, B. Jablonka, M. Just, J. Knolle, E. F. Paulus and G. Zoller, *J. Med. Chem.*, 1996, **39**, 2118–2122; C. Schnur, *J. Org. Chem.*, 1979, **44**, 3726–3727; F. C. Schaefer and G. A. Peters, *J. Org. Chem.*, 1961, **26**, 412–418; A. Thurkauf, *J. Labelled Compd. Radiopharm.*, 1997, **39**, 123–128; J. B. Kirby, N. A. van Dantzig, C. K. Chang and D. G. Nocera, *Tetrahedron Lett.*, 1995, **36**, 3477–3480; J. B. Medwid, *J. Med. Chem.*, 1990, **33**, 1230–1241.
7 V. Y. Kukushkin and A. J. L. Pombeiro, *Chem. Rev.*, 2002, **102**, 1771–1802.
8 J. Barker, M. Kilner, M. M. Mahmoud and S. C. Wallwork, *J. Chem. Soc., Dalton Trans.*, 1989, 837–841; S. Mazzega Sbovata, R. A. Michelin, M. Mozzon, A. Venzo, R. Bertani and F. Benetollo, *Inorg. Chim. Acta*, 2010, **363**, 487–494; S. Mazzega Sbovata, F. Bettio, C. Marzano, M. Mozzon, R. Bertani, F. Benetollo and R. A. Michelin, *Inorg. Chim. Acta*, 2008, **361**, 3109–3116; G. H. Sarova, N. A. Bokach, A. A. Fedorov, M. N. Berberan-Santos, V. Y. Kukushkin, M. Haukka, J. J. R. Frausto da Silva and A. J. L. Pombeiro, *Dalton Trans.*, 2006, 3798–3805; P. V. Gushchin, M. Haukka, N. A. Bokach and V. Y. Kukushkin, *Russ. Chem. Bull.*, 2008, **57**, 2125–2131; N. A. Bokach, T. V. Kuznetsova, S. A. Simanova, M. Haukka, A. J. L. Pombeiro and V. Y. Kukushkin, *Inorg. Chem.*, 2005, **44**, 5152–5160.
9 B. Longato, D. Montagner, G. Bandoli and E. Zangrando, *Inorg. Chem.*, 2006, **45**, 1805–1814.
10 D. Montagner, A. Venzo, E. Zangrando and B. Longato, *Inorg. Chem.*, 2010, **49**, 2103–2110.
11 M. N. Kopylovich and A. J. L. Pombeiro, *Coord. Chem. Rev.*, 2011, **255**, 339–355.

12 D. Montagner, E. Zangrando and B. Longato, *Inorg. Chem.*, 2008, **47**, 2688–2695.
13 L. Schenetti, A. Mucci and B. Longato, *J. Chem. Soc., Dalton Trans.*, 1996, 299–303.
14 E. G. Talman, W. Brüning, J. Reedijk, A. L. Spek and N. Veldman, *Inorg. Chem.*, 1997, **36**, 854–861.
15 T. J. Kistenmacher, M. Rossi, J. P. Caradonna and L. G. Marzilli, *Adv. Mol. Relax. Interact. Processes*, 1979, **15**, 119–133.
16 Z. Otwinowski and W. Minor, Processing of X-ray Diffraction Data Collected in Oscillation Mode, In *Methods in Enzymology*, ed. C. W. Carter Jr. and R. M. Sweet, Academic Press, New York, 1997, Vol. 276, p 307-326.
17 G. M. Sheldrick, *Acta Crystallogr., Sect. A: Found. Crystallogr.*, 2008, **64**, 112–122.
18 L. J. Farrugia, *J. Appl. Crystallogr.*, 1999, **32**, 837–838.
19 D. Montagner and B. Longato, *Inorg. Chim. Acta*, 2008, **361**, 1676–1680.
20 D. C. Prevorsek, *J. Phys. Chem.*, 1962, **66**, 769–778.
21 I. El Drubi Vega, P. A. Gale, M. E. Light and S. J. Loeb, *Chem. Commun.*, 2005, 4913–4915.
22 W. H. Press, B. P. Flannery, S. A. Teukolsky and W. T. Wetterling, *Numerical Recipies. The Art of Scientific Computing*, Cambridge U. P., Cambridge, 1986, p. 523.
23 G. G. Hammes and H. O. Spivey, *J. Am. Chem. Soc.*, 1966, **88**, 1621–1625; K. Yamamoto and N. Nishi, *J. Am. Chem. Soc.*, 1990, **112**, 549–558.
24 G. P. Johari and G. Sartor, *J. Phys. Chem. B*, 1997, **101**, 8331–8340.
25 D. Montagner, V. Gandin, C. Marzano and B. Longato, *J. Inorg. Biochem.*, 2011, **105**, 919–926.